2014 IEEE/RSJ International Conference on Intelligent Robots and Systems (IROS 2014)
September 14-18, 2014, Chicago, IL, USA

Optimal Dynamic Force Mapping for Obstacle-Aided Locomotion in 2D Snake Robots

Christian Holden[1], Øyvind Stavdahl[1] and Jan Tommy Gravdahl[1]

Abstract— **Snake robots are biomimetic robots highly suited for traversing challenging terrain where traditional robots have difficulty moving. A key aspect is obstacle-aided locomotion, where the snake pushes against the environment to achieve the desired propulsion. The main focus of this work is to optimally determine how to use the motor torque inputs that result in obstacle forces suitable to achieve some user-defined desired path for the snake. To this end, we present a new dynamical snake model, an explicit algebraic relationship between input and obstacle forces, and formulate an optimization problem that seeks to minimize energy consumption while achieving propulsion along the desired path.**

I. Introduction

Snake robots are biomimetic robots, designed to move in the same manner as biological snakes. In nature, snakes show remarkable adaptability in the different types of environments they can traverse. In addition to moving in highly unstructured environments, they can also swim, climb and – in some species – glide [1]. It is especially the ability to move efficiently in difficult terrain (dense forests, ruined buildings, etc.) where traditional wheeled or tracked robots have difficulty and flying robots can't go, that is interesting for snake robots. The ability to switch from one environment or propulsion mode to another (e.g., crawling to swimming) is also interesting. A machine capable of snake-like locomotion has a wide variety of applications, e.g., search-and-rescue, fire-fighting, inspection and exploration [2]–[4].

Conceptually, snake robots are n serially connected links, only attached to each other. Planar robots, such as the one discussed in this paper, therefore have $n + 2$ degrees of freedom (center of mass position and n rotation angles) and only $n - 1$ control inputs at the $n - 1$ joints. Unlike robot manipulators, they are therefore under-actuated. [2], [5]

Snake locomotion on smooth, usually flat, surfaces has been extensively studied (e.g., [2], [6]–[11]). Many real-life environments are not smooth, but cluttered. A key aspect of practical snake robots is therefore obstacle-aided locomotion, first defined by [12]. During this type of locomotion, the snake uses obstacles in the environment as push-points to propel itself forwards. This is common in nature [2]. Without proper use of obstacle-aided locomotion, snake robots lose their key advantage over other types of mobile robots, namely the ability to traverse a wide range of terrain.

Many authors, e.g., [2], [12]–[15], have presented models of snake robots in cluttered environments. These models are all of snakes with uniform links, and link centers of mass coinciding with the geometric center of the links. However, some snake robots do not conform to this, including a new experimental platform on which we hope to test novel control strategies [16]. Therefore, we have developed a new model, presented in this paper. The model is of a planar snake, with non-uniform links, and where the links' center of mass need not coincide with their geometric centers. This model is a more general form of that presented in [2, Ch. 2].

Obstacle-aided locomotion has been addressed in, among others, [2], [6], [13], [17]–[19]. Some of this research has been on shape-based control, where a basic motion pattern is propagated along the snake robot's body, and the pattern adjusted as necessary due to the presence of obstacles [2], [6], [17]. Other research has focused on asymmetric pushing against obstacles, with the pushing pattern fixed and determined *a priori* [18]; or on snake robots than can deform to exert extra push against the obstacles [13].

In this paper, we present a solution based on a different approach. The control of the snake robot is based on a hierarchical control structure (Fig. 1). We assume that trajectory planning for the snake's center of mass and head orientation (the first block in Fig. 1) has been done by higher-level control strategies or a human operator. The low-level control of individual joint angles is briefly touched upon, but not in detail, as this has been covered by previous authors (see, e.g., [2]). The component of the control hierarchy covered here is the second level, which deals with how to map a desired trajectory to obstacle contact forces, and these forces to control inputs.

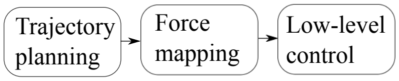

Fig. 1: Control hierarchy.

We determine an explicit, algebraic relationship between motor torques and obstacle forces, based on a fully dynamic model (unlike [19], which is based on static analysis). Since the number and nature of contact points between snake robot and obstacles changes discretely [2, Ch. 10], the relationship is only valid for single instances in time. The algebraic relationship is then updated on-line as the situation changes.

We use this relationship to determine the inputs that give the desired forces required to move the snake in the motion determined by the path planning algorithm or user, using an optimization criterion based on minimizing energy consumption (by proxy of the square of the motor torques),

[1] Department of Engineering Cybernetics, Norwegian University of Science and Technology, NO-7491 Trondheim, NORWAY. c.holden@ieee.org, oyvind.stavdahl@itk.ntnu.no, tommy.gravdahl@itk.ntnu.no

978-1-4799-6933-3/14/$31.00 ©2014 IEEE

while achieving the control goal. The optimization is by necessity performed on-line.

The main contributions of this paper are:

- A dynamical model for snakes with non-uniform links (Sec. III).
- *Main contribution:* An explicit, algebraic relationship between motor torque inputs and the resulting obstacle forces, based on the dynamical model (Sec. IV).
- *Main contribution:* The formulation of an optimization problem that uses the motor torque–obstacle force relationship to achieve a desired snake motion, while minimizing energy consumption (Sections VI and VII).
- A criterion for determining if a particular path can be used for snake locomotion (Sec. VI-A).

Currently, the user has to determine a path for the snake, a non-trivial task even with the suggested criterion. In our opinion, the search for an automatic way of doing this remains an important future challenge for obstacle-aided locomotion.

II. Nomenclature

The following notation is used in this work:

- Vectors are represented in a global, inertial reference frame where applicable.
- Vectors are written in lower-case, non-bold italics.
- Matrices are written in upper-case, non-bold italics.
- Elements of a vector are indicated with a subscript, e.g., x_2 is the second element of the vector x.
- The $\mathrm{diag}(\cdot)$ operator creates a diagonal matrix based on a vector argument.
- For the vector θ, $\sin(\theta)$ and $\cos(\theta)$ are the vectors of sines and cosines.
- As a shorthand, $\mathrm{s}_i = \sin(\theta_i)$ and $\mathrm{c}_i = \cos(\theta_i)$.
- Some vectors have, as a shorthand, defined matrix equivalents that are the diagonal matrices formed by the relevant vector. E.g., $M = \mathrm{diag}(m)$ where $m^{\mathrm{T}} = [m_1, \ldots, m_n]$.

A. The snake

See Fig. 2 for a visual representation of some of the parameters and variables listed here. Links are numbered from 1 (tail) to n (head).

1) Physical parameters: Physical parameters of the snake:

$n \geq 3 \in \mathbb{Z}$ Total number of links. There are $n-1$ joints.

$m_i \in \mathbb{R}$ Mass of link i. (Matrix: $M \in \mathbb{R}^{n \times n}$.)

$J_i \in \mathbb{R}$ Moment of inertia around the center of mass of link i. (Matrix: $J \in \mathbb{R}^{n \times n}$.)

$l_{h,i} \geq 0 \in \mathbb{R}$ Distance from the center of mass of link i to the next joint.

$l_{t,i} \geq 0 \in \mathbb{R}$ Distance from the center of mass of link i to the previous joint.

2) State variables: State variables of the snake robot:

$\theta_i \in \mathbb{R}$ Angle of link i relative to the inertial frame. (Vector: $\theta \in \mathbb{R}^n$.)

$x_i \in \mathbb{R}$ x-position of the center of mass of link i relative to the inertial frame. (Vector: $x \in \mathbb{R}^n$.)

$y_i \in \mathbb{R}$ y-position of the center of mass of link i relative to the inertial frame. (Vector: $y \in \mathbb{R}^n$.)

$p = [p_x, p_y]^{\mathrm{T}} \in \mathbb{R}^2$ Position of the snake's center of mass in the inertial frame.

3) Forces/moments: Forces and moments of the snake:

$u_i \in \mathbb{R}$ Motor torque on link i from the joint connecting links i and $i+1$. (Vector: $u \in \mathbb{R}^{n-1}$.)

$h_{x,i} \in \mathbb{R}$ Constraint force on link i from link $i+1$ in the global x-direction. (Vector: $h_x \in \mathbb{R}^{n-1}$.)

$h_{y,i} \in \mathbb{R}$ Constraint force on link i from link $i+1$ in the global y-direction. (Vector: $h_y \in \mathbb{R}^{n-1}$.)

$f_{x,i} \in \mathbb{R}$ Obstacle contact force on link i in the global x-direction. Zero for links not in contact with an obstacle. (Vector: $f_x \in \mathbb{R}^n$.)

$f_{y,i} \in \mathbb{R}$ Obstacle contact force on link i in the global y-direction. Zero for links not in contact with an obstacle. (Vector: $f_y \in \mathbb{R}^n$.)

$l_i \in [-l_{t,i}, l_{h,i}]$ Distance from the center of mass of link i to the point through which the contact force $[f_{x,i}, f_{y,i}]^{\mathrm{T}}$ is acting. $l_i = 0$ when the obstacle is in contact with the link's center of mass and (for simplicity) for links not in contact with obstacles. (Matrix: $L \in \mathbb{R}^{n \times n}$.)

$\tau_{r,i} \in \mathbb{R}$ Ground friction torque on link i. (Vector: $\tau_r \in \mathbb{R}^n$.)

$f_{r,x,i} \in \mathbb{R}$ Ground friction force on link i in the global x-direction. (Vector: $f_{r,x} \in \mathbb{R}^n$.)

$f_{r,y,i} \in \mathbb{R}$ Ground friction force on link i in the global y-direction. (Vector: $f_{r,y} \in \mathbb{R}^n$.)

B. Obstacles

Parameters of the obstacles:

$n_{\mathcal{C}} \geq 1 \in \mathbb{Z}$ Number of obstacles in contact with the snake.

$\gamma_i \in \{-1, 0, 1\}$ Indicates on which side of the link the obstacle is. For obstacles to the right of the link, $\gamma_i = 1$ and vice versa. Zero for links not in contact with an obstacle. (Vector: $\gamma \in \mathbb{R}^n$.)

$\bar{f}_i \in \mathbb{R}$ Signed magnitude of the obstacle force on link i. (Vector: $\bar{f}$.)

$g_{x,i} \in \mathbb{R}$ x-direction of the obstacle force on link i. $f_{x,i} = g_{x,i}\bar{f}_i$. (Matrix: $G_x \in \mathbb{R}^{n \times n}$.)

$g_{y,i} \in \mathbb{R}$ y-direction of the obstacle force on link i. $f_{y,i} = g_{y,i}\bar{f}_i$. (Matrix: $G_y \in \mathbb{R}^{n \times n}$.)

$f_{\mathcal{C}} \in \mathbb{R}^{nc}$ Vector of non-zero $\bar{f}_i$.

$P \in \mathbb{R}^{nc \times n}$ Selector matrix indicating which links are in contact with an obstacle. $f_{\mathcal{C}} = P\bar{f}$.

$\Gamma_{\mathcal{C}} \in \mathbb{R}^{nc \times nc}$ Matrix form of non-zero γ_i. $\Gamma_{\mathcal{C}} = \mathrm{diag}(P\gamma)$.

C. Control

Control variables:

$n_d \in [1, n)$ Number of links to be individually controlled.

$\theta_c \in \mathbb{R}^{n_d}$ Angles of the links to be individually controlled.

$\tilde{P} \in \mathbb{R}^{n_d \times n}$ Selector matrix indicating which links are to be individually controlled. $\theta_c = \tilde{P}\theta$.

$\theta_d \in \mathbb{R}^{n_d}$ Desired values for θ_c.

$p_{x,d} \in \mathbb{R}$ Desired x-position of the snake's center of mass.

$p_{y,d} \in \mathbb{R}$ Desired y-position of the snake's center of mass.

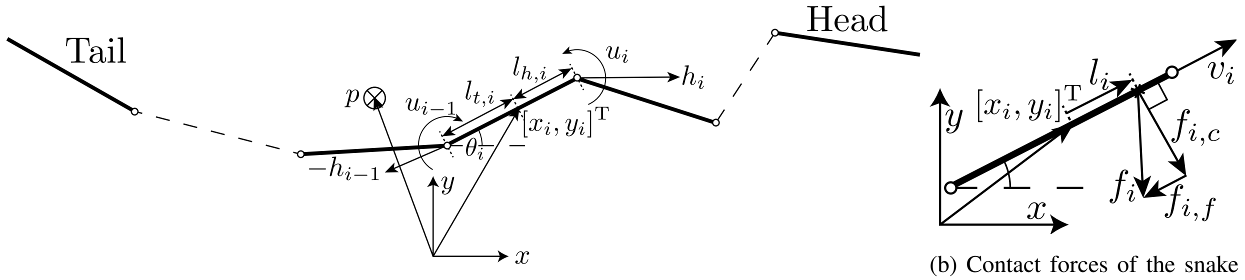

(a) Some parameters of the snake robot.

(b) Contact forces of the snake robot.

Fig. 2: Parameters of the snake robot.

D. Miscellaneous

Some constants and variables used throughout this work:

$$e^{\mathrm{T}} = [1, 1, \ldots, 1] \in \mathbb{R}^n \ , \quad E = ee^{\mathrm{T}} \in \mathbb{R}^{n \times n}$$

$$D = \begin{bmatrix} 1 & -1 & & 0 \\ & \ddots & \ddots & \\ 0 & & 1 & -1 \end{bmatrix} \in \mathbb{R}^{(n-1) \times n}$$

$$A_l = \begin{bmatrix} l_{h,1} & l_{t,2} & & 0 \\ & \ddots & \ddots & \\ 0 & & l_{h,n-1} & l_{t,n} \end{bmatrix} \in \mathbb{R}^{(n-1) \times n}$$

$$K_l = A_l^{\mathrm{T}} (DD^{\mathrm{T}})^{-1} D \in \mathbb{R}^{n \times n} \ , \quad \bar{m} = \frac{1}{n} \sum_{i=1}^{n} m_i \in \mathbb{R}$$

$$S_\theta = \mathrm{diag}(\sin(\theta)) \in \mathbb{R}^{n \times n} \ , \quad C_\theta = \mathrm{diag}(\cos(\theta)) \in \mathbb{R}^{n \times n}$$

$$Q_{\dot{\theta}} = \mathrm{diag}(\dot{\theta}) \in \mathbb{R}^{n \times n} \ , \quad \dot{\theta}^2 = \mathrm{diag}(\dot{\theta})\dot{\theta} \in \mathbb{R}^n \ .$$

Furthermore, I is the identity matrix of appropriate dimensions (usually $n \times n$). Note that $(DD^{\mathrm{T}})^{-1}$ always exists for $n \geq 2$ [2].

III. The dynamics of snake motion

To derive the equations describing the dynamics of the snake robot's motion and ensure a well-formulated problem, some assumptions have to be made:

1) The snake is planar.
2) All joints are actuated.
3) There are $n \geq 3$ links. The links may be non-identical. The centers of mass of the links do not need to be in the geometrical centers of the links.
4) Each link is touching at most one obstacle, and the snake at least one.
5) The obstacles are dimensionless; contact is at a single point.
6) Ground and obstacle friction can be modeled as coulomb friction. There is no stiction.
7) The links and the obstacles are perfectly rigid, and the obstacles immovable.
8) The desired trajectory of the snake's center of mass and the desired orientation of the snake's head are known and twice differentiable w.r.t. time.

The model that will be presented here is similar to that found in [2], but generalized to include non-identical links and rotational friction.

A. The dynamic equations

Extending [2, (2.11)] to non-uniform links gives the link positions

$$x = -K_l^{\mathrm{T}} \cos(\theta) + ep_x \tag{1}$$

$$y = -K_l^{\mathrm{T}} \sin(\theta) + ep_y \ . \tag{2}$$

These equations reflect the geometric relationship between the link centers of mass and the snake center of mass.

Taking the time derivatives of (1) and (2) gives the link velocities and accelerations

$$\dot{x} = K_l^{\mathrm{T}} S_\theta \dot{\theta} + e\dot{p}_x \tag{3}$$

$$\dot{y} = -K_l^{\mathrm{T}} C_\theta \dot{\theta} + e\dot{p}_y \tag{4}$$

$$\ddot{x} = K_l^{\mathrm{T}} C_\theta \dot{\theta}^2 + K_l^{\mathrm{T}} S_\theta \ddot{\theta} + e\ddot{p}_x \tag{5}$$

$$\ddot{y} = K_l^{\mathrm{T}} S_\theta \dot{\theta}^2 - K_l^{\mathrm{T}} C_\theta \ddot{\theta} + e\ddot{p}_y \ . \tag{6}$$

The translational dynamics of the links are given by

$$M\ddot{x} = f_{r,x} + f_x + D^{\mathrm{T}} h_x \tag{7}$$

$$M\ddot{y} = f_{r,y} + f_y + D^{\mathrm{T}} h_y \ . \tag{8}$$

Inserting (5), (6) into (7), (8) and solving for h_x and h_y gives

$$\begin{aligned} h_x = {} & (DD^{\mathrm{T}})^{-1} DMK_l^{\mathrm{T}} \left(C_\theta \dot{\theta}^2 + S_\theta \ddot{\theta} \right) \\ & - (DD^{\mathrm{T}})^{-1} D \left(f_{r,x} + f_x - Me\ddot{p}_x \right) \end{aligned} \tag{9}$$

$$\begin{aligned} h_y = {} & (DD^{\mathrm{T}})^{-1} DMK_l^{\mathrm{T}} \left(S_\theta \dot{\theta}^2 - C_\theta \ddot{\theta} \right) \\ & - (DD^{\mathrm{T}})^{-1} D \left(f_{r,y} + f_y - Me\ddot{p}_y \right) \ . \end{aligned} \tag{10}$$

The dynamics of the snake's center of mass follow Newton's Second Law; the time derivative of the momentum of the center of mass is equal to the sum of the external forces, or

$$n\bar{m}\ddot{p}_x = e^{\mathrm{T}}(f_{r,x} + f_x) \ , n\bar{m}\ddot{p}_y = e^{\mathrm{T}}(f_{r,y} + f_y) \ . \tag{11}$$

The rotational dynamics of the links are given by

$$\begin{aligned} J\ddot{\theta} = {} & D^{\mathrm{T}} u + \tau_r \\ & - S_\theta (A_l^{\mathrm{T}} h_x + L f_x) + C_\theta (A_l^{\mathrm{T}} h_y + L f_y) \ . \end{aligned} \tag{12}$$

Inserting (9) and (10) into (12), we get

$$\begin{aligned} J\ddot{\theta} = {} & D^{\mathrm{T}} u + \tau_r - \left[S_\theta K_l M K_l^{\mathrm{T}} S_\theta + C_\theta K_l M K_l^{\mathrm{T}} C_\theta \right] \ddot{\theta} \\ & - \left[S_\theta K_l M K_l^{\mathrm{T}} C_\theta - C_\theta K_l M K_l^{\mathrm{T}} S_\theta \right] \dot{\theta}^2 \\ & + S_\theta K_l \left(f_{r,x} + f_x \right) - C_\theta K_l \left(f_{r,y} + f_y \right) \\ & - S_\theta L f_x + C_\theta L f_y - S_\theta K_l M e\ddot{p}_x + C_\theta K_l M e\ddot{p}_y \end{aligned}$$

where we have used the definition of K_l.

Combining the above with the dynamics of the snake's center of mass, we get the total dynamics

$$\begin{aligned} M_\theta\ddot{\theta} &= D^{\mathrm{T}}u - W\dot{\theta}^2 + \tau_r - S_\theta L f_x + C_\theta L f_y \\ &\quad + S_\theta K_l \left(I - \frac{1}{n\bar{m}}ME\right)(f_{r,x} + f_x) \\ &\quad - C_\theta K_l \left(I - \frac{1}{n\bar{m}}ME\right)(f_{r,y} + f_y) \end{aligned} \tag{13}$$

$$n\bar{m}\ddot{p}_x = e^{\mathrm{T}}(f_{r,x} + f_x) \tag{14}$$

$$n\bar{m}\ddot{p}_y = e^{\mathrm{T}}(f_{r,y} + f_y) \tag{15}$$

where

$$\begin{aligned} M_\theta &= J + S_\theta K_l M K_l^{\mathrm{T}} S_\theta + C_\theta K_l M K_l^{\mathrm{T}} C_\theta \\ W &= S_\theta K_l M K_l^{\mathrm{T}} C_\theta - C_\theta K_l M K_l^{\mathrm{T}} S_\theta \ . \end{aligned}$$

We note that, if $m_i = \bar{m}$, $J_i = \bar{J}$ and $l_{h,i} = l_{t,i} = \bar{l}\ \forall\ i$, and $\tau_r = f_x = f_y = 0$; then the above equations would match [2, (2.33)].

IV. The obstacle force

The force acting on link i from an obstacle consists of two parts: one normal to the link and one tangent to the link. The normal force prevents the link from moving into the obstacle, and is the counter-force to the force with which the link is pushing against the obstacle (due to the action of the joint motors) by Assumption 7. The tangent force is due to friction. Let us define these forces as $f_{i,c} \in \mathbb{R}^2$ (constraint) and $f_{i,f} \in \mathbb{R}^2$ (friction), see Fig. 2b. Then, the obstacle force $f_i = [f_{x,i}, f_{y,i}]^{\mathrm{T}} \in \mathbb{R}^2$ is given by

$$f_i = f_{i,c} + f_{i,f} \ . \tag{16}$$

Let us assume that link i is pushing against an obstacle with a force of magnitude $\|\tilde{f}_i\|$, then $\|f_{i,c}\| = \|\tilde{f}_i\|$. If we define $\bar{f}_i \in \mathbb{R}$ as a "signed force magnitude" so that $|\bar{f}_i| = \|f_{i,c}\|$ and the sign of $\bar{f}_i$ indicates on which side of the obstacle link i is ($\bar{f}_i > 0$ for obstacles to the right of the link and vice versa), then the constraint force on link i from the obstacle will be given by

$$f_{i,c} = \bar{f}_i \begin{bmatrix} -\mathrm{s}_i \\ \mathrm{c}_i \end{bmatrix} \ . \tag{17}$$

To compute the friction, we need to know the velocity of the link at the point of contact with the obstacle. Let the position of the obstacle be $p_{o,i} \in \mathbb{R}^2$ in the inertial frame, $p_i^{\mathrm{T}} = [x_i, y_i] \in \mathbb{R}^2$ be the position of the center of mass of link i, and $p_{c,i} \in \mathbb{R}^2$ be the vector from the contact point to the center of mass of link i. Then,

$$p_{o,i} + p_{c,i} = p_i \ . \tag{18}$$

The obstacle's position is fixed in the inertial frame, so

$$\dot{p}_{o,i} = \dot{p}_i - \dot{p}_{c,i} = 0 \quad \Rightarrow \quad \dot{p}_{c,i} = \dot{p}_i \ . \tag{19}$$

We need the component of the velocity $\dot{p}_{c,i}$ that is tangent to the link, as only this will contribute to the friction. Let $v_{i,t} \in \mathbb{R}$ denote this component. Then,

$$v_{i,t} = [\mathrm{c}_i, \mathrm{s}_i]\dot{p}_{c,i} = \mathrm{c}_i\dot{x}_i + \mathrm{s}_i\dot{y}_i. \tag{20}$$

The friction will be proportional to the force with which link i is pushing against the obstacle (Assumption 6). Therefore,

$$\begin{aligned} f_{i,f} &= -\mu\|f_{i,c}\|\mathrm{sign}(v_{i,t}) \begin{bmatrix} \mathrm{c}_i \\ \mathrm{s}_i \end{bmatrix} \\ &= -\mu\,\mathrm{sign}(\bar{f}_i)\,\bar{f}_i\,\mathrm{sign}(v_{i,t}) \begin{bmatrix} \mathrm{c}_i \\ \mathrm{s}_i \end{bmatrix} \ . \end{aligned} \tag{21}$$

For convenience, we define $\tilde{\mu}_i \triangleq -\mu\,\mathrm{sign}(\bar{f}_i)\,\mathrm{sign}(v_{i,t})$ so that

$$f_i = f_{i,c} + f_{i,f} = \begin{bmatrix} \tilde{\mu}_i\mathrm{c}_i - \mathrm{s}_i \\ \tilde{\mu}_i\mathrm{s}_i + \mathrm{c}_i \end{bmatrix} \bar{f}_i \ . \tag{22}$$

Not all links are in contact with obstacles; for these links $\bar{f}_i = 0$. The vector $\bar{f} \in \mathbb{R}^n$ includes forces that are zero, while $f_{\mathcal{C}} = P\bar{f} \in \mathbb{R}^{nc}$ is the vector of only those signed force magnitudes that are non-zero. Furthermore,

$$g_{x,i} = \tilde{\mu}_i\mathrm{c}_i - \mathrm{s}_i \ , \quad g_{y,i} = \tilde{\mu}_i\mathrm{s}_i + \mathrm{c}_i$$

$$G_x = \mathrm{diag}([g_{x,1}, \ldots, g_{x,n}]) \in \mathbb{R}^{n\times n} \tag{23}$$

$$G_y = \mathrm{diag}([g_{y,1}, \ldots, g_{y,n}]) \in \mathbb{R}^{n\times n} \ , \tag{24}$$

so that

$$f_x = G_x P^{\mathrm{T}} f_{\mathcal{C}} \tag{25}$$

$$f_y = G_y P^{\mathrm{T}} f_{\mathcal{C}} \ . \tag{26}$$

Note that $f_{\mathcal{C}}$, like $\bar{f}$, contains *signed* values, and these signs must be preserved, as the sign indicates on which side of the obstacle the link is. Switching the sign would be equivalent to a link spontaneously moving to the other side of the obstacle. With γ_i as the correct sign of $\bar{f}_i$ and

$$\begin{aligned} \gamma &= [\gamma_1, \ldots, \gamma_n]^{\mathrm{T}} \in \mathbb{R}^n \\ \Gamma_{\mathcal{C}} &= \mathrm{diag}(P\gamma) \ , \end{aligned} \tag{27}$$

$f_{\mathcal{C}}$ must satisfy the constraint

$$\Gamma_{\mathcal{C}} f_{\mathcal{C}} \geq 0 \ . \tag{28}$$

We will show that $f_{\mathcal{C}}$ can be uniquely determined by the choice of u.

A. Finding $f_{\mathcal{C}}$

The links have to satisfy the non-holonomic constraint that the links' velocity component into the obstacles is zero (Assumption 7). Once again, $\dot{p}_{c,i} = \dot{p}_i$ is the velocity of the link at the point of contact. The normal component of this velocity, $v_{i,n} = [-\mathrm{s}_i, \mathrm{c}_i]\dot{p}_i \in \mathbb{R}$ has to satisfy

$$\gamma_i v_{i,n} \geq 0 \ . \tag{29}$$

Since $\gamma_i = 0$ for links not in contact with obstacles, this is trivially satisfied for those links. For the links that are in contact with an obstacle, this presents a genuine constraint.

To simplify the analysis, we make the following observation: If a link is in contact with an obstacle, the force it can generate will either help the snake move in the desired manner or it won't; in the latter case we should not let the snake push against it (the resultant force from that obstacle is then zero). However, obstacles that are currently not helpful may be so in the future, as the desired motion might change. As such, links that are in contact with obstacles should remain so (but we should not necessarily push against them).

We therefore choose the constraints to be

$$\gamma_i v_{i,n} = 0 \; . \tag{30}$$

In other words, we will use control action u to enforce a stricter constraint (30) than is enforced by the model (29).

We now write the constraints vectorially. Let $v_n = [v_{1,n}, \ldots, v_{n,n}] \in \mathbb{R}^n$. Eq. (30) gives $Pv_n = 0 \in \mathbb{R}^{nc}$, or

$$Pv_n = -PS_\theta \dot{x} + PC_\theta \dot{y} = 0 \; . \tag{31}$$

To find the forces arising from this constraint, we need the time derivative of (31); the constraint forces arise from the equation [20, Ch. 6]

$$\frac{\mathrm{d}Pv_n}{\mathrm{d}t} = 0 \; . \tag{32}$$

As long as the snake does not lose/gain contact with any obstacles, $\frac{\mathrm{d}Pv_n}{\mathrm{d}t} = P\frac{\mathrm{d}v_n}{\mathrm{d}t}$. Using (5) and (6), we find

$$\begin{aligned}
\frac{\mathrm{d}v_n}{\mathrm{d}t} &= -S_\theta \ddot{x} - C_\theta Q_{\dot{\theta}} \ddot{x} + C_\theta \ddot{y} - S_\theta Q_{\dot{\theta}} \dot{y} \\
&= -\left(S_\theta K_l^{\mathrm{T}} S_\theta + C_\theta K_l^{\mathrm{T}} C_\theta\right) \ddot{\theta} - S_\theta e \ddot{p}_x + C_\theta e \ddot{p}_y \\
&\quad - C_\theta \left(Q_{\dot{\theta}} K_l^{\mathrm{T}} - K_l^{\mathrm{T}} Q_{\dot{\theta}}\right) S_\theta \dot{\theta} - C_\theta \dot{\theta} \dot{p}_x \\
&\quad + S_\theta \left(Q_{\dot{\theta}} K_l^{\mathrm{T}} - K_l^{\mathrm{T}} Q_{\dot{\theta}}\right) C_\theta \dot{\theta} - S_\theta \dot{\theta} \dot{p}_y \; .
\end{aligned} \tag{33}$$

For convenience, we define

$$\tilde{M}_\theta = S_\theta K_l^{\mathrm{T}} S_\theta + C_\theta K_l^{\mathrm{T}} C_\theta \; , \tilde{K}_l = Q_{\dot{\theta}} K_l^{\mathrm{T}} - K_l^{\mathrm{T}} Q_{\dot{\theta}} \; .$$

Inserting the dynamics (13)–(15) into (33) and premultiplying with P, we rewrite (32) as

$$A_f f_{\mathcal{C}} + A_u u = b_f \tag{34}$$

where $A_f \in \mathbb{R}^{nc \times nc}$, $A_u \in \mathbb{R}^{nc \times (n-1)}$ and $b_f \in \mathbb{R}^{nc}$ are given by

$$\begin{aligned}
A_f &= P\left(\tilde{M}_\theta M_\theta^{-1} \tilde{G} + \frac{1}{n\bar{m}}\left(S_\theta E G_x - C_\theta E G_y\right)\right) P^{\mathrm{T}} \\
\tilde{G} &= S_\theta \left(K_l \left(I - \frac{1}{n\bar{m}} ME\right) - L\right) G_x \\
&\quad - C_\theta \left(K_l \left(I - \frac{1}{n\bar{m}} ME\right) - L\right) G_y \\
A_u &= P\tilde{M}_\theta M_\theta^{-1} D^{\mathrm{T}} \\
b_f &= -P\tilde{M}_\theta M_\theta^{-1} \left(\tau_r + S_\theta K_l \left(I - \frac{1}{n\bar{m}} ME\right) f_{r,x}\right) \\
&\quad + P\tilde{M}_\theta M_\theta^{-1} \left(W\dot{\theta}^2 + C_\theta K_l \left(I - \frac{1}{n\bar{m}} ME\right) f_{r,y}\right) \\
&\quad - \frac{1}{n\bar{m}} PS_\theta E f_{r,x} + \frac{1}{n\bar{m}} PC_\theta E f_{r,y} \\
&\quad - P\left(C_\theta \tilde{K}_l S_\theta - S_\theta \tilde{K}_l C_\theta + \dot{p}_x C_\theta + \dot{p}_y S_\theta\right) \dot{\theta} \; .
\end{aligned}$$

We note that, assuming A_f to be invertible, the inequality constraint (28) can be rewritten as a constraint on u, namely

$$\Gamma_{\mathcal{C}} A_f^{-1} A_u u \leq \Gamma_{\mathcal{C}} A_f^{-1} b_f \; . \tag{35}$$

V. Final dynamical equation

We can now rewrite the dynamical equations for the snake:

$$\begin{aligned}
M_\theta \ddot{\theta} &= Bu - W\dot{\theta}^2 + g_r & (36)\\
n\bar{m}\ddot{p}_x &= e^{\mathrm{T}} \left(f_{r,x} + G_x P^{\mathrm{T}} A_f^{-1} \left(b_f - A_u u\right)\right) & (37)\\
n\bar{m}\ddot{p}_y &= e^{\mathrm{T}} \left(f_{r,y} + G_y P^{\mathrm{T}} A_f^{-1} \left(b_f - A_u u\right)\right) & (38)
\end{aligned}$$

where $B \in \mathbb{R}^{n \times (n-1)}$ and $g_r \in \mathbb{R}^n$ are given by

$$\begin{aligned}
B &= D^{\mathrm{T}} - \tilde{G} P^{\mathrm{T}} A_f^{-1} A_u \\
g_r &= \tau_r + S_\theta K_l \left(I - \frac{1}{n\bar{m}} ME\right) f_{r,x} \\
&\quad - C_\theta K_l \left(I - \frac{1}{n\bar{m}} ME\right) f_{r,y} + \tilde{G} P^{\mathrm{T}} A_f^{-1} b_f
\end{aligned}$$

subject to

$$\Gamma_{\mathcal{C}} A_f^{-1} A_u u \leq \Gamma_{\mathcal{C}} A_f^{-1} b_f \; . \tag{39}$$

Note that the matrices A_f, A_u, G_x, G_y, P, $\Gamma_{\mathcal{C}}$ and the vector b_f will change depending on which links are in contact with obstacles. This will change over time, as discrete events, and the equations are only valid as long as this does not occur.

The dynamics of the snake forms a hybrid system; a new set of equations of similar structure but with different values for the matrices will be valid after the discrete event. This is in accordance with the results of [2, Ch. 10]. No effort is here made to model the transitions, as this is not necessary for the optimization algorithm and thus beyond the scope of this work.

VI. Control objective

The primary objective is to get the snake to move in the desired direction. We express this as a desired path for the snake's center of mass and a desired head angle, assumed known (Assumption 8).

In order to achieve this, external forces have to be present. In this case, that is predominantly achieved from pushing against obstacles. As the angle of the link determines the direction of the obstacle force (22), links that are in contact with obstacles might need to maintain a certain angle to achieve desired direction of the force. If a link is in contact with an obstacle and the snake moves, the link will at some point leave the obstacle. It may therefore be considered useful to also angle the following link so that it will hit the obstacle at the right angle.

It is possible to demand specific behavior of other links. However, this would reduce redundancy. Furthermore, it is largely unnecessary; only the behavior of the snake at or near obstacles is likely to have a significant effect on the propulsion of the snake. Other links contribute only via friction, which is likely to be dominated by the obstacle forces, and would largely be the same no matter the configuration of the snake between obstacles.

Let us formalize the control objective.

We define the error between the angles we wish to control θ_c and the desired values for these angles θ_d (assumed known, Assumption 8) as $\tilde{\theta} = \theta_c - \theta_d \in \mathbb{R}^{n_d}$. We find

$$\ddot{\tilde{\theta}} = \tilde{P} M_\theta^{-1} \left(Bu - W\dot{\theta}^2 + g_r \right) - \ddot{\theta}_d \, . \tag{40}$$

We define the error between the actual position of the snake's center of mass $[p_x, p_y]$ and the desired position $[p_{x,d}, p_{y,d}]$ (assumed known, Assumption 8) as $\tilde{p}_x = p_x - p_{x,d} \in \mathbb{R}$ and $\tilde{p}_y = p_y - p_{x,d} \in \mathbb{R}$. We find

$$\ddot{\tilde{p}}_x = \frac{1}{n\bar{m}} e^{\mathrm{T}} \left(f_{r,x} + G_x P^{\mathrm{T}} A_f^{-1} \left(b_f - A_u u \right) \right) - \ddot{p}_{x,d} \tag{41}$$

$$\ddot{\tilde{p}}_y = \frac{1}{n\bar{m}} e^{\mathrm{T}} \left(f_{r,y} + G_y P^{\mathrm{T}} A_f^{-1} \left(b_f - A_u u \right) \right) - \ddot{p}_{y,d} \tag{42}$$

The low-level control action u (Fig. 1) gives the closed-loop dynamics

$$\ddot{\tilde{\theta}} = f_{\tilde{\theta}}(\tilde{\theta}, \dot{\tilde{\theta}}, t) \tag{43}$$

$$\ddot{\tilde{p}}_x = f_{\tilde{p}_x}(\tilde{p}_x, \dot{\tilde{p}}_x, t) \tag{44}$$

$$\ddot{\tilde{p}}_y = f_{\tilde{p}_y}(\tilde{p}_y, \dot{\tilde{p}}_y, t) \, . \tag{45}$$

The precise nature of $f_{\tilde{\theta}}$, $f_{\tilde{p}_x}$ and $f_{\tilde{p}_x}$ are determined by the low-level controller.

Regardless of the precise functional expressions, we can insert the desired dynamics (43)–(45) into the actual dynamics (40)–(42), and rewrite the equations as

$$A_e u = b_e \tag{46}$$

where $A_e \in \mathbb{R}^{(2+n_d)\times(n-1)}$ and $b_e \in \mathbb{R}^{2+n_d}$ are given by

$$A_e = \begin{bmatrix} e^{\mathrm{T}} G_x P^{\mathrm{T}} A_f^{-1} A_u \\ e^{\mathrm{T}} G_y P^{\mathrm{T}} A_f^{-1} A_u \\ \tilde{P} M_\theta^{-1} B \end{bmatrix}$$

$$b_e = \begin{bmatrix} e^{\mathrm{T}} \left(f_{r,x} + G_x P^{\mathrm{T}} A_f^{-1} b_f \right) - n\bar{m}(f_{\tilde{p}_x} + \ddot{p}_{x,d}) \\ e^{\mathrm{T}} \left(f_{r,y} + G_y P^{\mathrm{T}} A_f^{-1} b_f \right) - n\bar{m}(f_{\tilde{p}_y} + \ddot{p}_{y,d}) \\ \tilde{P} M_\theta^{-1} \left(W\dot{\theta}^2 - g_r \right) + f_{\tilde{\theta}} + \ddot{\theta}_d \end{bmatrix} .$$

The control input would be any u that satisfies (46). (Note that this holds true no matter which low-level controller is chosen.) We describe a method for choosing a specific u in Sec. VII, and a simple low-level controller in Sec. VI-B.

A. Path quality

A pertinent question is under what conditions (46) has a solution. This is not trivial to answer, and will depend on the configuration of the snake and the number and position of the obstacles. While it is fairly easy to check numerically to see if a particular configuration allows a solution to (46) (e.g., by the Rouché-Capelli Theorem [21]), an analytical criterion would rapidly become cumbersome.

At least in part, the problem also depends on the choice of path, as the situation at the links in contact with the obstacles is largely determined by the path the head took earlier. A perfectly controlled snake robot is analogous to a train: the path are the tracks, the head the locomotive, and the other links the railcars; the rail cars/links must follow the same path as the locomotive/head link. Of course, the snake will not be perfectly controlled in practice, but the analogy is often a useful abstraction. As mentioned previously, automatically finding a good or even feasible path is an unsolved problem, beyond the scope of this work, and assumed generated by the first block of Fig. 1 (a human operator or future algorithms).

However, a method for checking the quality of a chosen path (i.e., its suitability for locomotion) presents itself: The existence of a solution to the equation $A_e u = b_e$, under the constraint $\Gamma_{\mathcal{C}} A_f^{-1} A_u u \leq \Gamma_{\mathcal{C}} A_f^{-1} b_f$, implies that useful forces can be generated. If a solution exists no matter where on the path the snake is, then the path will be traversable.

This can be investigated off-line.

B. Low-level control design

Design of the low-level controller (Fig. 1) is not the main focus of the paper, and largely beyond the scope of this work. None the less, we here present a simple low-level controller capable of achieving the control goal. Refinement or design of a better controller remains future work.

Let

$$f_{\tilde{\theta}}(\tilde{\theta}, \dot{\tilde{\theta}}, t) = -K_{p,\theta}\tilde{\theta} - K_{d,\theta}\dot{\tilde{\theta}} \tag{47}$$

$$f_{\tilde{p}_x}(\tilde{p}_x, \dot{\tilde{p}}_x, t) = -k_{p,x}\tilde{p}_x - k_{d,x}\dot{\tilde{p}}_x \tag{48}$$

$$f_{\tilde{p}_y}(\tilde{p}_y, \dot{\tilde{p}}_y, t) = -k_{p,y}\tilde{p}_y - k_{d,y}\dot{\tilde{p}}_y \tag{49}$$

where $k_{p,x}, k_{d,x}, k_{p,y}, k_{d,y} > 0 \in \mathbb{R}$, $K_{p,\theta}, K_{d,\theta} > 0 \in \mathbb{R}^{n_d \times n_d}$ are controller gains. Then, assuming (46) can be solved for u, the closed-loop dynamics are given by

$$\ddot{\tilde{p}}_x + k_{p,x}\tilde{p}_x + k_{d,x}\dot{\tilde{p}}_x = 0 \tag{50}$$

$$\ddot{\tilde{p}}_y + k_{p,y}\tilde{p}_y + k_{d,y}\dot{\tilde{p}}_y = 0 \tag{51}$$

$$\ddot{\tilde{\theta}} + K_{p,\theta}\tilde{\theta} + K_{d,\theta}\dot{\tilde{\theta}} = 0 \tag{52}$$

which, with appropriate choices for the controller gains, have an exponentially stable equilibrium at the origin. (This is a feedback linearizing controller.)

VII. Optimization

Given that there will most likely exist more than one solution to the control equation (46), it seems prudent to choose one that minimizes the energy consumption of the snake. For convenience, we use a weighted sum of the squares of the joint torques u_i as a proxy.

So far in the paper, we have described several constraints that need to be satisfied. These are: that links cannot spontaneously move to the other side of the obstacles, represented by (39); that links should not move away from obstacles and that the control objective is satisfied, both covered by (46). In this section we also add a new constraint based on the maximum torques of the motors.

Optimization Problem 1: For any time instant t, minimizing the energy cost while ensuring that the snake moves in the desired direction can be done by solving the following quadratic programming problem:

$$\min_{u,z} u^{\mathrm{T}} Q_u u + z^{\mathrm{T}} Q_z z \tag{53}$$

$$\text{s.t.} \quad \Gamma_{\mathcal{C}} A_f^{-1} A_u u \leq \Gamma_{\mathcal{C}} A_f^{-1} b_f \tag{54}$$

$$A_e u + z = b_e \tag{55}$$

$$|u_i| \leq u_{i,\max} \; \forall \, i \in \{1, \ldots, n-1\} \tag{56}$$

where $z \in \mathbb{R}^{2+n_d}$ are slack variables; and $Q_u \geq 0 \in \mathbb{R}^{(n-1)\times(n-1)}$ and $Q_z \geq 0 \in \mathbb{R}^{(2+n_d)\times(2+n_d)}$ are weighting matrices. $\triangle$

We note that this problem is a convex quadratic programming problem, and as such will have a unique globally optimal solution. Algorithms for solving such problems are fast and readily available in a wide variety of software packages. We also note that while the precise numerical values of $\Gamma_{\mathcal{C}}$, A_f, A_u, b_f, A_e and b_e change depending on system state, desired path and the chosen low-level controller, the optimization problem still remains fundamentally the same; for each time step we simply use the new, updated values.

If the optimal slack variables z are not very small, then the desired trajectory is not achievable in the current snake/obstacle configuration and the trajectory planning (Fig. 1) was poor.

VIII. Numerical results

The ideal test (other than experimental verification) of the optimization problem suggested in this paper, would be to test the snake's ability to traverse a simulated, cluttered environment. However, this necessitates some method – preferably automatic – of determining the desired angles θ_d and trajectory $[p_{x,d}, p_{y,d}]^{\mathrm{T}}$. As previously discussed, the creation of an automatic method is non-trivial and an active area of research, and beyond the scope of this paper.

Instead, a simple demonstration of the optimization problem, for a single frozen moment in time, on a virtual snake robot, is presented to illustrate the algorithm.

The specifics of the ground friction has so far been of little interest. For the numerical calculations, we used coulomb friction with friction coefficients μ_g (linear ground friction $f_{r,x}$, $f_{r,y}$) and $\mu_{g,r}$ (rotational ground friction τ_r).

Table I defines the physical constants of the snake (link sizes but not the arbitrarily selected weights match the robot of [16]). Table II contains the current state of the snake, and Table III the number and placement of the obstacles. The control parameters are listed in Table IV. In this example, the snake is currently in a sinusoidal pattern, in contact with five obstacles. The center of mass is moving slowly, and the desired position of the snake's center of mass is 1 m to the right.

The optimal parameters found can be seen in Table V and illustrated in Fig. 3. In Fig. 3, obstacles are drawn as circles. Crosses represent the joints on the snake, and the crossed circles indicate link centers of mass. The head is to the right. Constraint forces $f_{i,c}$ are dashed, while actual contact forces f_i (includes obstacle friction) are solid. The forces indicated

TABLE I: Parameters used.

Prameter	Value	Unit
n	20	–
$m_i, i < n$	1	kg
m_n	2	kg
$J_i, i < n$	0.001	kg·m^2
J_n	0.0015	kg·m^2
$l_{h,i}, i < n$	0.0233	m
$l_{h,n}$	0.0117	m
$l_{t,i}, i < n$	0.0617	m
$l_{t,n}$	0.0628	m
g	9.81	m/s^2
μ_g	0.3	–
$\mu_{g,r}$	0.1	–
μ	0.3	–
Q_u	I	(N·m)$^{-2}$
Q_z	$10^{12} I$	s^4/m^2
$u_{i,\max}$	4.5	N·m

TABLE II: Current state.

Var.	Value	Unit	Var.	Value	Unit
θ	$\begin{bmatrix} 0.8631 \\ 0.8631 \\ 0.4144 \\ -0.2731 \\ -0.8777 \\ -1.1165 \\ -0.8777 \\ -0.2731 \\ 0.4144 \\ 0.8631 \\ 0.8631 \\ 0.4144 \\ -0.2731 \\ -0.8777 \\ -1.1165 \\ -0.8777 \\ -0.2731 \\ 0.4144 \\ 0.8631 \\ 0.8631 \end{bmatrix}$	rad	$\dot{\theta}$	$\begin{bmatrix} 0.4655 \\ 0.0616 \\ -0.4594 \\ -1.0177 \\ -1.0615 \\ -0.3505 \\ 1.0203 \\ 0.9696 \\ 0.7274 \\ 0.2561 \\ -0.6099 \\ -1.0676 \\ -1.2700 \\ -0.4941 \\ 1.2480 \\ 1.4646 \\ 1.2580 \\ 0.7426 \\ 0.2983 \\ -0.1065 \end{bmatrix}$	rad/s
p^{T}	0	m	$\dot{p}^{\mathrm{T}}$	$[0.1625, 0.0244]$	m/s

TABLE III: Obstacles.

Variable	Value	Unit
$n_{\mathcal{C}}$	5	–
l_i	0	m
$P_{1,3} = P_{2,6} = P_{3,10}$ $= P_{4,14} = P_{5,18}$	1	–
Other $P_{i,j}$	0	–
$P\gamma$	$[-1, 1, -1, 1, -1]^{\mathrm{T}}$	–

TABLE IV: Control objective.

Parameter	Value	Unit
$p_{x,d}$	1	m
$p_{y,d}$	0	m
$\tilde{P}_{1,1} = \tilde{P}_{2,3} = \tilde{P}_{3,4} = \tilde{P}_{4,6} = \tilde{P}_{5,7} = \tilde{P}_{6,10}$ $= \tilde{P}_{7,11} = \tilde{P}_{8,14} = \tilde{P}_{9,15} = \tilde{P}_{10,18} = \tilde{P}_{11,19}$	1	–
Other $\tilde{P}_{i,j}$	0	–
θ_d	$\tilde{P}\theta$	rad
$\dot{\theta}_d$	0	rad/s
$\dot{p}_{x,d} = \dot{p}_{y,d}$	0	m/s
$\ddot{p}_{x,d} = \ddot{p}_{y,d}$	0	m/s^2
$k_{p,x} = k_{p,y} = k_{d,x} = k_{d,y}$	1	Multiple
$K_{p,\theta} = K_{d,\theta}$	I	Multiple

are those obtained from the optimization. Forces are scaled, reduced by a factor of 1:105.

As we can see, the optimization algorithm is, for this configuration, able to find a globally optimal solution. Using MATLAB 2013b on a laptop with a 2.3 GHz Intel Core i7 processor, the algorithm completes in approx. 0.1 s; implemented in a compiled language such as C it is expected to be several magnitudes faster.

TABLE V: Optimization results.

Par.	Value	Unit
u^{T}	$[1.029, 3.217, 3.939, 1.014, -2.644, -4.500, -1.728,$ $1.192, 3.131, 3.776, 3.776, 2.408, 0.228, -2.836,$ $-4.117, -1.922, 0.300, 1.898, 2.191, 1.250]$	N·m
$\lVert z \rVert_2$	$< 10^{-11}$	m/s^2
$f_{\mathcal{C}}^{\mathrm{T}}$	$[\ -25.450, 50.577, -18.634, 27.276, -11.920\ ]$	N

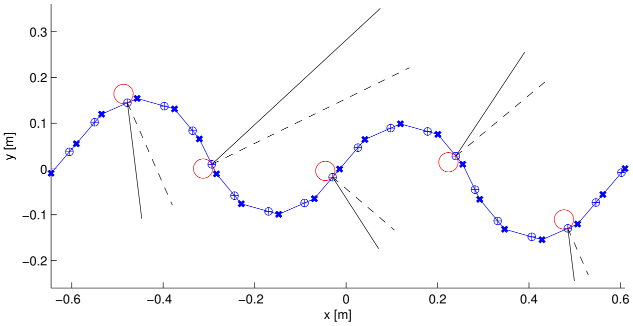

Fig. 3: Optimization results. Circular obstacles, $f_{i,c}$ dashed, f_i solid. Forces are scaled 1:105.

IX. Conclusions

This paper has investigated a solution to a fundamental problem in snake locomotion: how to best utilize obstacles in the environment as push-points to achieve desired locomotion.

To investigate this problem, we present a model of non-uniform snake robots in contact with obstacles and find an explicit, algebraic relationship between motor torque inputs and obstacle forces.

Using the input–obstacle force relationship, we present a method for obstacle-aided locomotion. Given any system state, a desired path, and desired angles for some of the links, the optimization problem we present (a convex quadratic programming problem) minimizes energy (by proxy of the square of the motor torques), given the constraint that the control goal is to be satisfied.

Assuming there is a feasible solution, the optimization problem is easily solvable by existing algorithms. As a by-product, the existence of feasible solutions can be used to determine, off-line, if a path is suitable for locomotion or not, something that has until now been difficult to determine.

The solution presented here is an important step on the road to practical obstacle-aided locomotion; however, there are two key issues that remains future work. First, an automatic method for finding the desired link angles at the obstacles, given the desired path (these reference angles are currently assumed user-supplied). Second, given a specific environment, an automatic method of finding the desired path (also, currently assumed user-supplied). These are major, ongoing areas of research in snake robotics.

Acknowledgements

This work was supported by the Research Council of Norway through the SLICE project, project number 205622.

References

[1] H. Cogger and R. Sweifel, *Reptiles & Amphibians*. Weldon Owen, 1992.

[2] P. Liljebäck, K. Y. Pettersen, Ø. Stavdahl, and J. T. Gravdahl, *Snake Robots – Modelling, Mechatronics, and Control*. Springer, 2012.

[3] S. Hirose and E. F. Fukushima, "Snakes and strings: New robotic components for rescue operations," *Int. J. of Robotics Research*, vol. 23, no. 341–349, 2004.

[4] P. Liljebäck, Ø. Stavdahl, and A. Beitnes, "SnakeFighter – development of a water hydrolic fire fighting snake robot," in *Proc. IEEE Int. Conf. on Control, Automation, Robotics and Vision*, 2006.

[5] P. Liljebäck, K. Y. Pettersen, Ø. Stavdahl, and J. T. Gravdahl, "Controllability and stability analysis of planar snake robot locomotion," *IEEE Trans. on Automatic Control*, vol. 56, no. 6, pp. 1365–1380, 2011.

[6] S. Hirose, *Biologically Inspired Robots*. Oxford Univ. Press, 1993.

[7] J. Ostrowski and J. Burdick, "The geometric mechanics of undulatory robotic locomotion," *Int. J. of Robotics Research*, vol. 17, no. 7, pp. 683–701, 1998.

[8] J. Burdick, J. Radford, and G. Chirkjian, "A "sidewinding" locomotion gait for hyper-redundant robots," in *Proc. 1993 IEEE Int. Conf. Robotics and Automation*, vol. 3, 1993, pp. 101–106.

[9] M. Saito, M. Fukaya, and T. Iwasaki, "Serpentine locomotion with robotic snakes," *IEEE Control Systems Magazine*, vol. 22, no. 1, pp. 64–81, 2002.

[10] G. Chirkjian and J. Burdick, "The kinematics of hyper-redundant robot locomotion," *IEEE Trans. on Robotics and Automation*, vol. 11, no. 6, pp. 781–793, 1995.

[11] K. Lipkin, I. Brown, A. Peck, H. Choset, J. Rembisz, P. Gianfortoni, and A. Naaktgeboren, "Differentiable and piecewise differentiable gaits for snake robots," in *Proc. 2007 IEEE/RSJ Int. Conf. Intelligent Robotos and Systems*, 2007, pp. 1864–1869.

[12] A. A. Transeth, R. Leine, C. Glocker, K. Y. Pettersen, and P. Liljebäck, "Snake robot obstacle aided locomotion: modeling, simulations and experiments," *IEEE Trans. on Robotics*, vol. 24, no. 1, pp. 88–104, 2008.

[13] Z. Bayraktaroglu and P. Blazevic, "Understanding snakelike locomotion through a novel push-point approach," *J. Dynamical Systems, Measurment and Control*, vol. 127, no. 1, pp. 146–152, 2005.

[14] H. Date and Y. Takita, "Adaptive locomotion of a snake like robot based on curvature derivatives," in *Proc. IEEE/RSJ Int. Conf. on Intelligent Robots and Systems*, 2007, pp. 3554–3559.

[15] I. Tanev, T. Ray, and A. Buller, "Automated evolutionary design, robustness and adaption of side-winding locomotion of a simulated snake-like robot," *IEEE Trans. on Robotics*, vol. 21, no. 4, pp. 632–645, 2005.

[16] P. Liljebäck, Ø. Stavdahl, K. Y. Pettersen, and J. T. Gravdahl, "A modular and waterproof snake robot joint mechanism with a novel force/torque sensor," in *Proc. IEEE/RSJ Int. Conf. on Intelligent Robots and Systems*, 2012, pp. 4898–4905.

[17] Z. Bayraktaroglu, "Snake-like locomotion: experimentations with a biologically inspired wheel-less snake robot," *Mechatronics and Machine Theory*, vol. 44, no. 3, pp. 591–602, 2008.

[18] T. Kamegawa, R. Kuroki, M. Travers, and H. Choset, "Proposal of EARLI for the snake robot's obstacle aided locomotion," in *Proc. 2012 IEEE Int. Symp. on Safety, Security and Rescue Robotics*, 2012.

[19] C. Holden and Ø. Stavdahl, "Optimal static propulsive force for obstacle-aided locomotion in snake robots," submitted to the 2013 IEEE Int. Conf. on Robotics and Biomimetics.

[20] F. Udwadia and R. Kalaba, *Analytical Dynamics: A New Approach*. Cambridge Univ. Press, 1996.

[21] A. Carpinteri, *Structural Mechanics*. Taylor and Francis, 1997, p. 74.